



Wissenschaftlicher Ergebnisbericht / Scientific Report 2003

Schwerpunkt / main research area
FE-Vorhaben / RD project
Institutsbeitrag / institute's contribution

Energie / Energy
E04 Nukleare Sicherheitsforschung
51201
Geschäftsbereich Sicherheit und Strahlenschutz /
Department for Safety and Radiation Protection (S)
Dr. R. Hille r.hille@fz-juelich.de
Nuclear Safety Research
Safety Research for Nuclear Waste Disposal
www.fz-juelich.de/scientific-report

Verantwortlich / in charge
HGF-Forschungsbereich / Research Field
HGF-Programm / Programme
HGF-Thema / Topic
Internet

Detailergebnisse / Details

AN ASSESSMENT OF THE LONG-TERM EVOLUTION OF 'EFFECTIVE' SOIL CONTAMINATION

DEDERICHS H., HILL P., LENNARTZ R., PILLATH J., HILLE R.

Abstract

After the accident at Chernobyl in 1986 the time dependent development of the environmental contamination and of population doses was investigated by several national and international institutions. This contribution presents results obtained in a recent study of the long-term evaluation of contamination carried out in Belarus at two municipalities of Korma county.

The directly measured external dose rate was twice as high as the calculated dose rate of measured soil contamination. Therefore it was necessary to define the 'effective' soil contamination. This includes additionally to the pure soil the plant part as radiation source, where the plant part consists of roots with humic acid bound radionuclides. Measurements show that 14 years after the accident on the average 24.5% of the total activity whereas on the average only 9.8% of the total weight was in the plant part.

To calculate the long-term evolution of the 'effective' soil contamination an semi-empirical assessment procedure was developed. It consists of a set of two differential equations with three parts. The first part considers the radioactive decay, the second considers residence near the surface (0cm-10cm), and the third is concerned with retransfer to plants and their roots with humic acid bound.

The solutions of differential equations show exponential formulas. Generally the migrating activity is the dominant part during the first years, but this changes with time in favour of the retransfer part. Details depend as well on the type and treatment of soil as on the type of biotope. The activity increases in the organic layer to a maximum after twenty to thirty years. Thereafter the decay defines the decreasing slope of the curve. In wooded regions the retransferred part is dominant after one year, compensating the vertical migration. The decrease of activity in the upper layer is only defined by the decay.

1. Introduction

In the first years after the Chernobyl accident, the internal dose fraction was dominant for the total radiation exposure of the population in the radioactively highly contaminated regions. Especially in smaller, secluded places at the edge of the confiscated zones, where the population's self-supply fraction of nutrition plays an essential role, this is the case even today.

As a rule, however, the external dose is predominant. Comparisons of the external dose determined, on the one hand, by air dose rate measuring instruments and calculated, on the other hand, from soil contamination sometimes show similarly different values. This applies, in particular, to extensively vegetated areas and forest regions. Botsch (2000) also found in his investigations that, contrary to expectations, no linear correlation can be observed between soil contamination and measured area dose rates. These differences show that the calculation of external doses from soil contamination taking the activity distribution in the soil and on the soil surface over vegetated areas into consideration does not yet lead to satisfactory results and requires further investigations.

To this purpose, investigations were carried out in the Korma district (Belarus) to determine the external dose both from air dose rate measurements and from soil contamination, and a simple procedure was developed to describe the correlations between area dose rate and soil contamination taking the biological components into consideration. First results are reported in this conference contribution, a more detailed paper will be published elsewhere¹.

2 Taking soil samples

The collection of soil samples was performed according to the German guideline on emission and immission monitoring of nuclear facilities (Der Umweltminister, 1993). Each collection site was a square area with a side length of 5 m, from which a sample was taken at each of the four corner points and in the centre of the square. The five samples thus taken were mixed and then regarded as an averaging sample for the collection site. In addition to the pure earth mass, the organic matter such as low plants, mosses, grasses and herbs as well as their root systems contained in the drill head was separately collected, weighed and spectrometrically measured. Comparing the sample masses taken, organic component and mineral soil samples, and their activity it is found that the organic component comprises 24.5% \pm 8.1% of the total activity measured, although the mass is only 9.4% \pm 3.7% of the total mass. The organic component is more highly contaminated by a factor of three than the pure soil and thus keeps the contamination high in the top layers and at the soil surface. The fraction of activity bound by humic acids in the upper soil layer could not be determined.

3 A semi-empirical assessment for determining the time dependent contamination

An assessment will be presented, which globally describes this phenomena and permits an analytical calculation of the contamination profile in the soil taking all migration and transfer effects into account. Schell et al. (1996 and 2001) described the contamination profile in forests by a differential equation system consisting of six interlinked equations, with which they determined the activity in trees, in underwood, in the organic soil layer, in an up to 80 cm deep soil layer, in which the activity bound to roots, on the one hand, the activity chemically bound to earth, on the other, and the migration into deeper layers are described. For a general description of the contamination profile it would be advisable to reduce the equation system in such a way that an analytical solution can be obtained.

For this purpose, the following basic assumptions are made:

Migration is regarded as an ensemble without differentiating the detailed distribution and diffusion in the soil. It represents a quantity averaged over the whole land area concerned. The depth band of migration is to consider as a physical continuum.

The transfer of activity and its binding in and to plants is considered for the ensemble of all plants in total, so that this quantity also represents an averaging in terms of a retransfer. Thus the retransfer is the average reflow of activity from the continuum. The fact that the plants also bind part of the contamination in a defined surface layer is suppressed in the model, in that the thickness of this surface layer is regarded as infinitesimally small. In this way, the activity sum of soil contamination and organic component can be defined as "effective" surface contamination.

The annual die-off of the plants is not regarded as a new source term. This effect is incorporated in the constants to be used. Although trees and shrubbery also take the activity from deeper soil layers and bring it to the surface again by shedding their leaves, this is not considered as an additional source term either. This effect is covered by averaging the migration and retransfer.

A decrease in activity due to possible soil erosion need not be taken into account since it is negligibly small.

Figure 1 shows a scheme of the activity fluxes of the model. The constants in figure 1 have the following meaning:

¹ Dederichs H.; Pillath J.; Lennartz R.; Hill P.; Hille R.; *Specifics of the temporal development of the radioactivity distribution in the ground and of the area dose rate in the Korma district, Belarus, 15 years after the Chernobyl accident*; submitted to Kerntechnik

$$\lambda_m = 1/n \sum_{i=1}^n \lambda_{m_i} \quad [a^{-1}] \text{ the averaged migration constant,}$$

$$\lambda_T = 1/n \sum_{i=1}^n \lambda_{T_i} \quad [a^{-1}] \text{ the averaged retransfer constant and}$$

$$\lambda_z \quad [a^{-1}] \text{ the radioactive decay constant.}$$

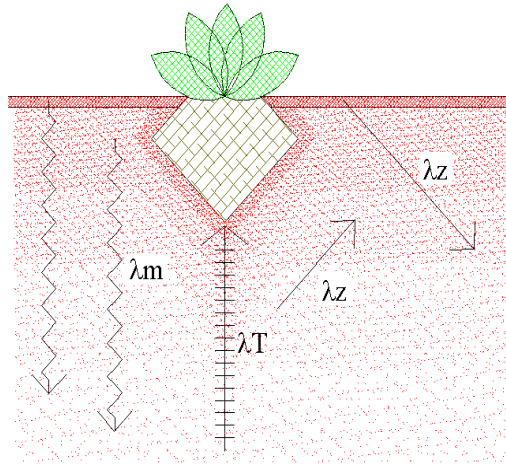


Figure 1: The scheme of assessment

Taking the simplifying assumptions into consideration, two interlinked differential equations can be generated, one for the "effective" surface contamination $N(t)$, that part of the contamination which is directly located at the surface together with the organically bound activities, and one for the migrating fraction $M(t)$ without depth differentiation.

The solution of that differential equations gives the variation in time of the effective surface contamination:

$$N(t) = N_0 e^{-\lambda_z t} [(\lambda_m e^{-(\lambda_m + \lambda_T) t} + \lambda_T) / (\lambda_m + \lambda_T)]$$

Analogously to the solution approach of effective surface contamination, the solution of the variation in time of the migrating fraction is obtained:

$$M(t) = N_0 e^{-\lambda_z t} \lambda_m / (\lambda_m + \lambda_T) (1 - e^{-(\lambda_m + \lambda_T) t})$$

In this assessment, as already mentioned before, the migrating component and the retransfer of the "effective" surface contamination are treated as a large-area and temporal mean value. Furthermore, the equations are only valid for a once-only contamination, which is given by the starting conditions $N(t=0)=N_0$ and $M(t=0)=0$. Though the deposition of radionuclides after Chernobyl accident might have extended over a time period of several days, it can be considered as a one time event with respect to the long term evaluation of "effective" contamination.

4 Application of the assessment

The procedure for calculating the variation in time of the "effective" surface contamination for ^{137}Cs can be demonstrated by the example of the municipality of Volincy. The municipality of Volincy is situated in the forest belt of the Korma district.

The soil samples of the villages of the municipality were measured with and without plant vegetation. Since retransfer is only applied to the organic component, the retransfer constant $\lambda_T = 0$ can be substituted in the equation for the "effective" surface contamination in determining the "pure" soil sample. The values specified on Belarusian contamination maps of 1991 are also regarded as values without organic component. If the equation is applied without retransfer and solved for λ_m , the averaged migration constant is obtained. The surface contamination N_0 can also be determined with this equation. The values for λ_m and N_0 determined in this way can now be used to iteratively fit the retransfer constant λ_T .

Figure 2 shows the normalized average variation in time of the "effective" ^{137}Cs surface contamination of the municipality of Volincy as well as the curve of the derived activity bound to and in plants.

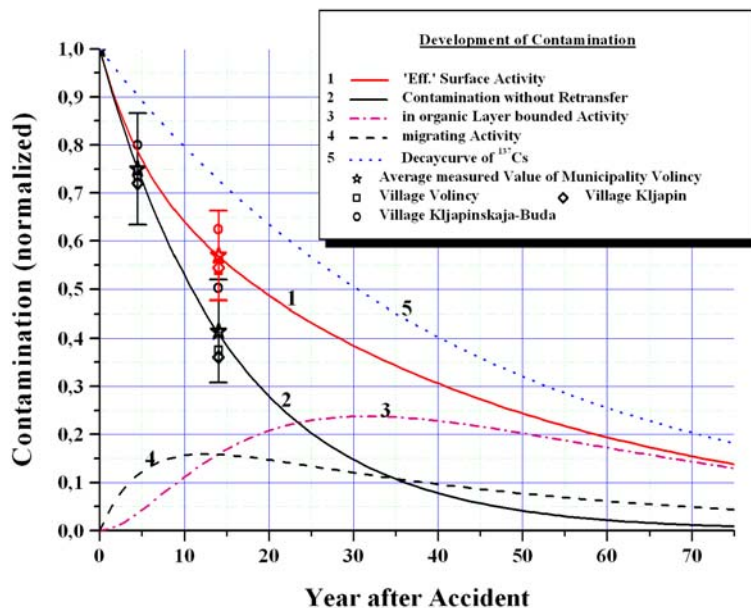


Figure 2: Normalized averaged variation of the "effective" surface contamination of the municipality of Volincy.

The curve behaviour for the municipality of Volincy shows that the large retransfer in comparison to migration keeps the "effective" surface contamination high. This means that the activity bound in and to plants accounts for the major portion of total activity in the course of further development. It steadily increases in the first few years (curve 3) and reaches its maximum after about 30 years.

A higher averaged migration constant is to be expected for intensively tilled agricultural areas. Figure 3 shows the normalized average variation in time of the "effective" ^{137}Cs surface contamination of the municipality of Vornovka, an agriculturally intensively used region.

A comparison of averaged variation of the "effective" surface contamination of both municipalities shows for the pure agricultural region Vornovka a higher migration of ^{137}Cs activity and lower retransfer.

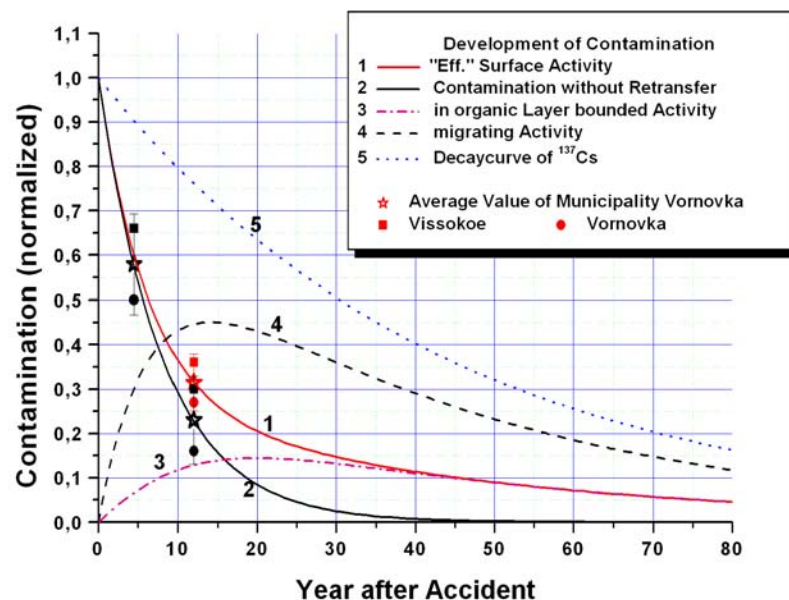


Figure 3: Normalized averaged variation of the "effective" surface contamination of the municipality of Vornovka.

As can be seen from the preceding diagrams, a value of 15% of the initial activity is still to be expected with constant vegetation even after long time, although the "pure" soil contamination has nearly vanished which means that rest activity is bound in and to organic components. The decrease in "effective" soil contamination now takes place almost exclusively via radioactive decay. This is illustrated very well by a comparison of the decay curve with the solid curve of "effective" surface contamination.

Figure 4 shows the normalized averaged variation in time of the "effective" ^{137}Cs surface contamination in the forest as well as the course of the derived activity bound to and in plants and trees.

Although only one soil sample from the forest of the Strumen confiscated zone was available, an attempt to describe the temporal development of the ^{137}Cs forest contamination was carried out. The “effective” soil contamination measurement was backed up by numerous measurements of the area dose rate in the forests of the Korma region. The contamination of trees and shrubs was also determined with the aid of measurements of the area dose rates. It amounted to $15.8 \pm 2.4 \%$ of total contamination.

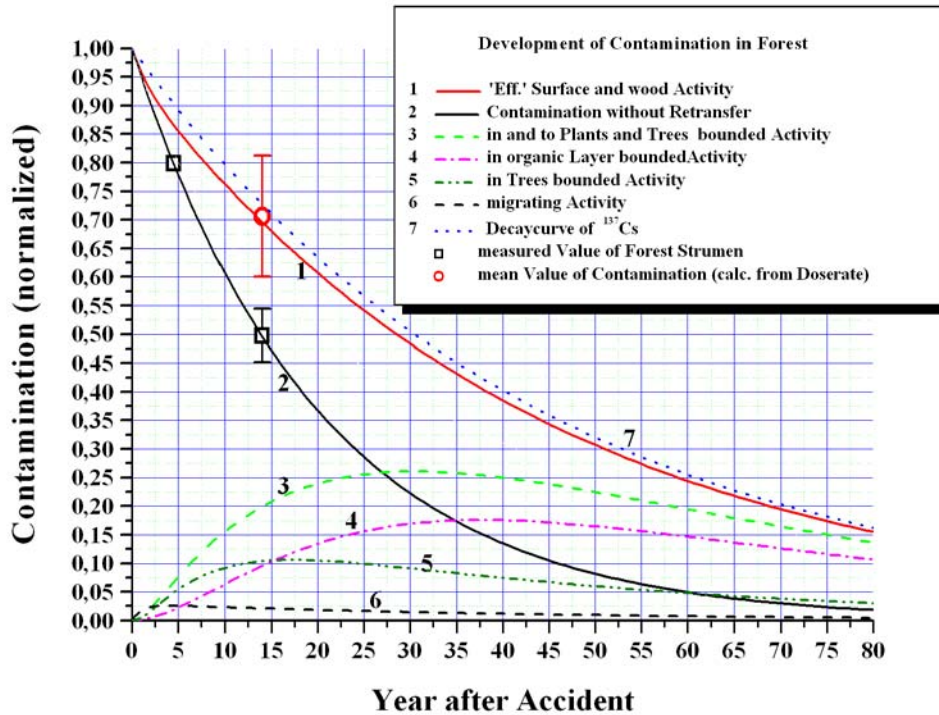


Figure 4: Normalized time-averaged variation of the contamination in forest Strumen

It can be seen from Figure 4 that the ^{137}Cs contamination in the forest regions of the Korma district decreases almost exclusively via radioactive decay. The migrating fraction is almost negligibly small. It reaches its maximum of 2.5% of the ^{137}Cs initial activity after approx. three years. This is different for the activity bound in trees and in and to organic matter. It reaches its maximum of 27% of the initial activity after approx. thirty years and decreases slowly. Its rise to the maximum is determined by the activity bound in the tree stand. This initially rises relatively rapidly and reaches its maximum of approx. 12% after approx. fifteen years. The organically bound fraction increases with a time lag and reaches its maximum of 18% after approx. thirty-five years.

The accumulation of radionuclides in forest ecosystems is specified by several authors for the same period of time. According to Schell et al. (2001) the maximum concentration in trees is reached after

15 years, according to Shaw et al. (1996) after 12.5 years, and Tikhomirov et al. (1991-1992) predicted the highest contamination value in the tree stand after 10-12 years.

5 Conclusion

With the empirically determined constants, the assessment described reflects the variation in time of the "effective" surface contamination with sufficient accuracy. It takes migration and retransfer into account as the ensemble of all the effects involved. If the retransfer constant is set equal to zero, the solution of the model is simplified into known equations so far derived from measured values for the variation in time of soil contamination.

Retransfer is found to be a quantity that can not be neglected. This applies, in particular, to prolonged periods of time after the contaminating event. Above a certain level of the retransfer constant this means that the decrease in contamination is then mainly determined by radioactive decay. The main component of the activity is bound in this case in and to organic matter, in detail:

1. maximum of activity bound in organic layer
 - for pure agricultural region ca. 15% after ca. 20 years,
 - for forestal regions ca. 24% after ca. 30 years,
 - for forest's ca. 17% after ca. 40 years (with tree bound activity ca. 27% after ca. 30 years)
2. after 15 years the activity bound in organic layer will be the dominant part of contamination
3. the decrease after maximum of activity bounded in organic layer is defined by radioactive decay

If these results are generally taken as a basis for forest regions, the consequence would be that the Cs incorporation currently observed for wild boars (Umwelt, 2001), which find their nutrition on the ground and in the top soil layers, will rise for approx. another 15 years, provided that the vegetation remains the same kind. A further observation of the body burden of wild boars may be helpful for validating the semi-empirical assessment of this paper.

References

Botsch, W. (2000). *Untersuchungen zur Strahlenexposition von Bewohnern hochkontaminierter Ortschaften in der nördlichen Ukraine*. PhD thesis, Centre for Radiation Protection and Radioecology of the University of Hanover, May 2000

Der Umweltminister, (1993). *Richtlinie zur Emissions- und Immissionsüberwachung kerntechnischer Anlagen*. GMBI No. 29, 502,

- Schell, W.R., Linkow, I., Myttenaere, C., Morel, B. (1996). *A Dynamic Model For Evaluating Radionuclide Distribution In Forest From Nuclear Accident*, Health Physics 70 (3): 318-335,
- Schell, W.R., Linkow, I. (2001). *Transfer in forest ecosystems*. In Radioecology (edit. by E. Van der Stricht, R. Kirchmann), Oupeye, Belgium, ISBN 2-9600316-0-1
- Shaw, G., Kliastorin, A., Mamikhin, S., Shcheglov, A., Rafferty, B., Dvornik, A.M., Zhuchenko T.A. (1996). *Modelling radiocesium fluxes in forest ecosystems*, Proceedings of the 1st International Conference on Radiological Consequences of the Chernobyl Accident (pp. 221-224), Minsk, Belarus, 18-22 March 1996
- Tikhomirov, F. et al. (1991-1992). *Radionuclides migration in natural and semi-natural ecosystems*, Report 1991-1992, C.E.C. Project ECP-5, Doc. ENEA-DISP/ARA-MET, 6, (pp. 49-108)
- Umwelt. (2001). *Tschernobyl-Cäsium in Waldökosystemen*, Journal Umwelt, 762, 11/2001

Induction of complex DNA double strand breaks by incorporated Auger electron emitters²

E. Pomplun

INTRODUCTION

Since more than three decades it is well known that Auger electron emitting radionuclides can induce severe chromatin damage if they decay within or near the DNA molecule [1, 2]. Different mechanisms have been made responsible for this so-called 'Auger effect': (a) the great number of low-energy and short-ranging Auger electrons released during the nuclide's decay, (b) the chemical transmutation to the daughter element, (c) the recoil energy of the nucleus, and also (d) a 'Coulomb explosion' due to the highly charged daughter atom and subsequent repulsion between the atoms of the molecule. In the meantime many experimental and theoretical work have contributed to elucidate the effective mechanisms.

In this report the role of the Auger electrons will be highlighted by modelling the physical and physico-chemical phase of the radiation action mechanism. During this early period the initial spectrum of primary events (ionisations, excitations) and species (radicals) is produced which determines the final biological effect. In particular, the effectiveness of the two Auger electron emitters ¹²³I and ¹²⁵I will be compared here, because this comparison allows to cancel out the transmutation effect since both isotopes decay to tellurium. Also the influence from the Coulomb explosion should be the same for both so that the differences in biological effectiveness can be attributed to the different Auger electron spectra only.

In vitro survival experiments have demonstrated a significant difference in cell killing efficiency showing ¹²⁵I to be 2.3 times more toxic than ¹²³I at the D₃₇-level [3]. To understand this difference on the molecular scale the Auger electron spectra must be known as well as the number and spatial distribution of initial ionisations and radical species and their reactions with the critical target(s). These processes have been simulated with Monte Carlo methods. The energy depositions by the electrons and subsequently the tracks' interactions with a DNA nucleosome model have been converted into strand breaks of different complexity (for details see [4]). Differences in the experimental survival curves between both isotopes should be reflected by differences in the break patterns.

² Data from this report have partially been published in: Pomplun, Terrissol and Hille, Radiat. Prot. Dosim.

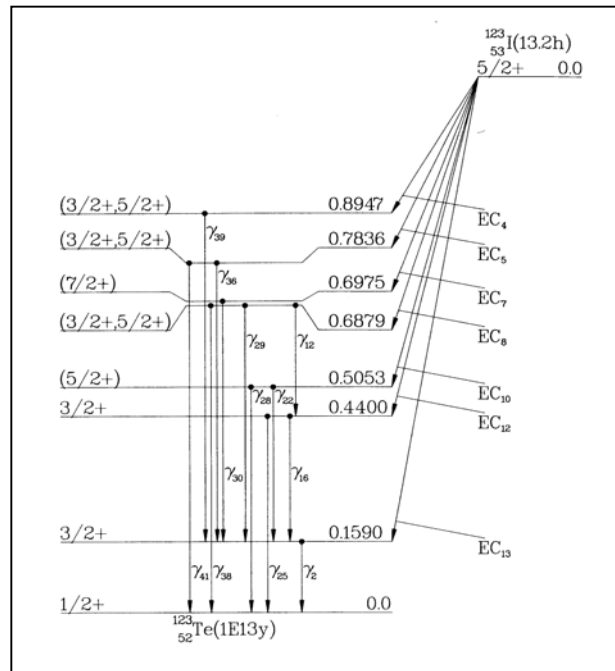


Figure 1: Decay scheme of ^{123}I

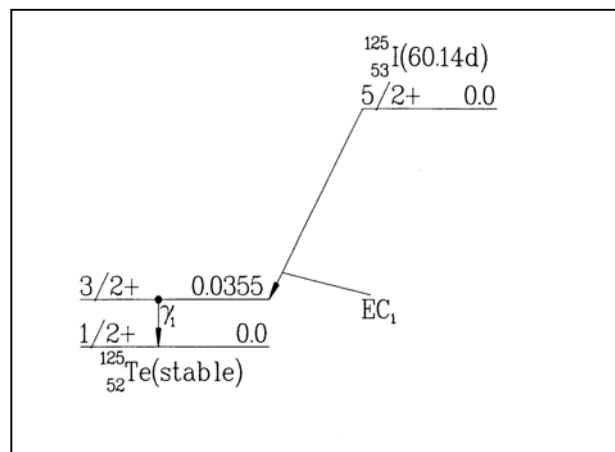


Figure 2: Decay scheme of ^{125}I

METHODS

The decay mechanisms of ^{123}I and ^{125}I (Figures 1 and 2) have been simulated to generate electron spectra for individual decays. A modified version of a Monte Carlo computer code could be used here [5], strongly adapted to experimental noble gas data. These electron spectra provide the data base for track structure calculations in combination with a DNA nucleosome model (Figure 3) to assess the radiolytic efficiency and the DNA strand break pattern distribution [4].

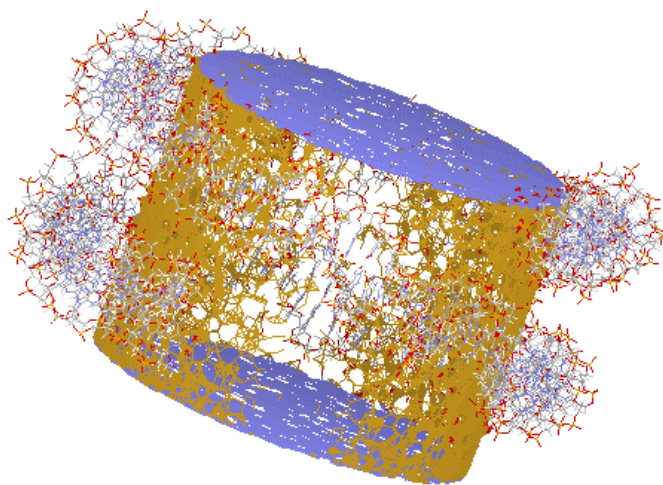


Figure 3: DNA nucleosome model (the cylinder represents the histons' volume)

The complete modelling system includes the following features: (a) MC simulation of the ^{123}I and ^{125}I Auger cascades, (b) four-dimensional (x,y,z,t) electron transport in liquid water, (c) a DNA nucleosome model with three-dimensional atomic coordinates (see Figure 3), (d) liquid water ionisations and excitations, direct effects in the DNA at 10^{-15} s, (e) diffusion of all water radicals and reactions amongst themselves and with sub-units of the DNA as a function of time, (f) scoring of indirect effects in the DNA between 10^{-12} to 10^{-8} s. For details of spectra generation, track structure simulation and break pattern assessment see [4 –7].

RESULTS

Charge Distributions and Auger Electron Spectra: Both nuclides decay by electron capture followed by internal conversion or gamma emission, respectively. However, differences in gamma emission probabilities lead to different numbers of released electrons (see Figure 4). For ^{123}I a mean number of 8.5 Auger and conversion electrons has been calculated with a maximum of 25, whereas 15 and 30 are the correspondent numbers for ^{125}I .

Primary Products: From the survival experiment [3] the D_{37} -level has been chosen as the common biological endpoint for both nuclide's radiation. In case of ^{125}I , 120 decays are necessary, in case of ^{123}I 277 decays to reduce the number of proliferating cells to this level. For these decay numbers the primary products have been evaluated (see Table 1). For both isotopes the figures are in the same or

der of magnitude, however, a ratio of cell killing effectiveness reported from the experiment ($277 / 120 = 2.3$) cannot be deduced from these data.

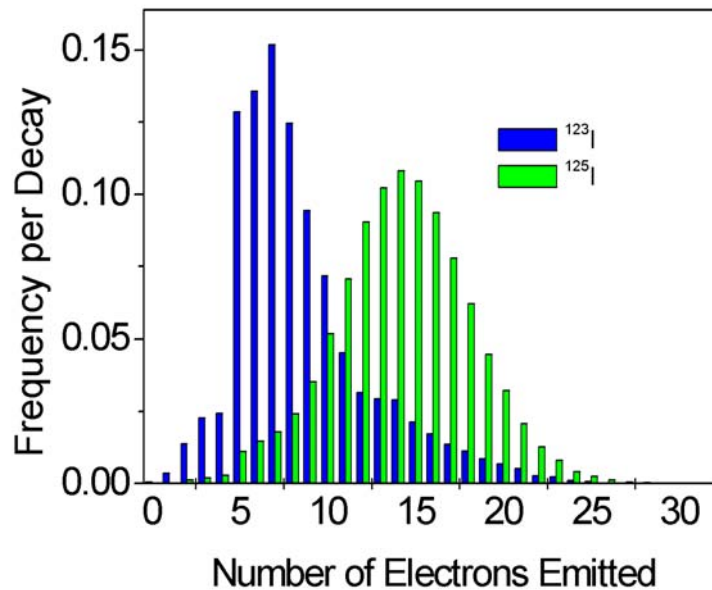


Figure 4: Frequency distribution of emitted electron numbers

Products	120 Decays of ^{125}I UdR	277 Decays of ^{123}I UdR
Primary events (phys. Phase)		
	~ 49 200	~ 58 200
	~ 34 800	~ 41 500
Ionisations in cell nucleus	~ 1 320	~ 1 660
	~ 840	~ 1 100
Excitations in cell nucleus		
Ionisations in DNA		
Excitations in DNA		
Radicals in cell nucleus (after 10^{-12} s)		
OH^\cdot	~ 70 800	~ 83 100
e^-_{aq}	~ 64 800	~ 77 600
H^\cdot	~ 8 400	~ 9 400

Table 1: Products in mammalian cell nucleus after decays of DNA-bound ^{123}I and ^{125}I

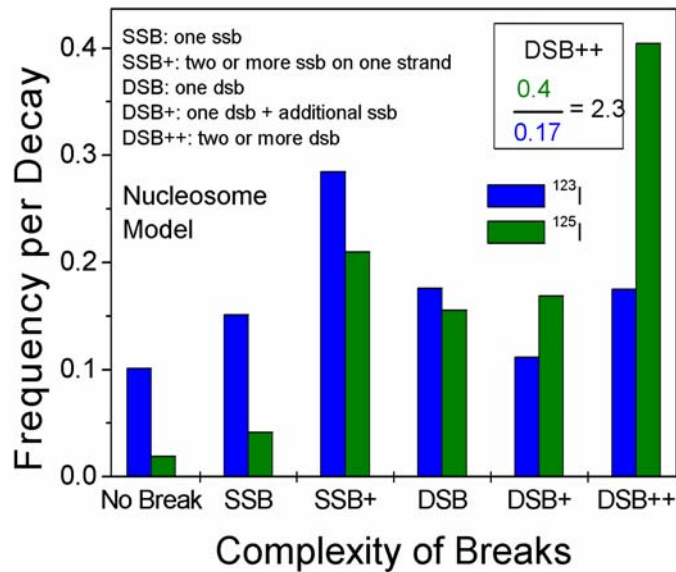


Figure 5: Distributions of DNA strand break patterns (SSB: single strand break, DSB: double strand break)

Break Patterns: A spectrum of break patterns is shown in Figure 5. It gives the relative frequencies for different types of breaks as a function of their complexity. From earlier investigations [4] it can be concluded that complex break patterns correspond with high energy depositions whereas 'No break' or simple 'SSB' resulted from low energy depositions. The distributions of the break patterns differ strongly between ^{123}I and ^{125}I . Whereas for ^{125}I 'DSB++' is the most frequent break type (in about 40% of all ^{125}I decays), ^{123}I produces mainly 'SSB+' (28%). Considering only the most complex type of breaks ('DSB++') at the end of the chemical stage (10^{-8} s), the same ratio ($0.404 / 0.175 = 2.3$) is seen as in the survival experiment [3].

DISCUSSION

It is certainly not surprising that a single 'mean' decay of ^{123}I is clearly less radiotoxic than a 'mean' ^{125}I decay, because ^{123}I emits only about half the number of electrons compared to ^{125}I . Interesting, however, is the fact that the same ratio of severe double strand breaks ('DSB++') has been found here by modelling as it can be derived from experiments on cell survival. This suggests that these very complex DNA breaks are strongly associated with cell killing.

REFERENCES

- [1] Hofer KG, Hughes WL. Radiotoxicity of intranuclear tritium, ^{125}I iodine and ^{131}I iodine. Radiat Res 1971; 47:94-109.

- [2] Feinendegen LE, Ertl HH, Bond VP. Biological toxicity associated with the Auger effect. In: Ebert H, editor, Proceedings of the Symposium on Biophysical Aspects of Radiation Quality. Vienna: IAEA, 1971: 419-430.
- [3] Makrigiorgos, G.M., Kassis, A.I., et al., *Radiotoxicity of 5-[¹²³I]Iodo-2'-deoxyuridine in V79 cells: a comparison with 5-[¹²⁵I]Iodo-2'-deoxyuridine*, Radiat. Res. 118, 532-544 (1989)
- [4] Pomplun, E. and Terrissol, M. *Low-energy electrons inside active DNA models: a tool to elucidate the radiation action mechanisms*, Radiat. Environ. Biophys. 33, 279-292 (1994)
- [5] Pomplun, E. *Auger electron spectra – the basic data for understanding the Auger effect*, Acta Oncologica 39, 673-679 (2000)
- [6] Terrissol, M. and Beaudre, A. *Simulation of space and time evolution of radiolytic species induced by electrons in water*, Radiat. Prot. Dosim. 31, 175-177 (1990)
- [7] Terrissol, M., Demonchy, M. and Pomplun, E. *A new approach to radiation transport in the complex DNA environment*, in: Microdosimetry, pp. 15-18, Goodhead DT et al. (Eds.), The Royal Society of Chemistry, Special Publication No. 204, Cambridge 1997

